DEFORMATION OF A PERFECT DIELECTRIC DROP IN ELECTRO-OSMOTIC FLOW OF AN ELECTROLYTE THROUGH A MICROCHANNEL

Chemical Engineering Research Project – CHEN90023
Department of Chemical and Biomolecular Engineering
University of Melbourne

Michelle Felisberto
Student Number: 747049

November 2015

Contents

1 Abstract

This research project studies the motion and deformation of a perfect dielectric drop in a microchannel filled with an electrolyte solution. The behavior of the drop in electro-osmotic flow was modelled numerically using a computational dynamic fluid model. The influence of varying wall charge density, the Debye-Huckel parameter and the Weber number are considered for uncharged, positively and negatively charged drop interfaces. The electro-osmotic flow of the fluid and drop are analyzed, as well as the drop deformation under low surface tension conditions. The influence of charge distribution, electric field and permittivity jump on drop velocity and deformation were also discussed. It was found that for a positively charged channel wall, negatively charged drops move faster and positively charged drops move slower compared to when there is no interface charge on the drop. This effect was enhanced for a higher Weber number. A vortex flow was observed inside the drop as a result of electrical forces acting on the surface of the drop. The increase in wall charge density was proven to enhance the effects of drop mobility but showed little effect on drop deformation. For the case with sufficiently low surface tension, some deformation was observed on the drop due to permittivity and charge forces acting on the drop surface. The positively and negatively charged drops deformed more than the uncharged drop due to the greater effect of charge forces surrounding the drop. This effect was amplified further when the permittivity force component was removed by making drop and continuous fluid permittivity equal. In fact it was sufficiently high to cause the negatively charged drop to break up.

2 Introduction

The fundamental understanding of electro-osmotic flow of liquids and electrical properties in microchannels is an important subject of study in many areas, such as biochemical and chemical analysis and emulsions. This is present in numerous applications, such as soil remediation [1], lab-on-a-chip [2] and electro-osmotic pumps [3]. An important part of these studies are focused on predicting the behavior of droplets in microfluidic and nanofluidic applications, especially regarding the colloid industry [4].

Various numerical models have been developed to describe these microsystems accounting for electro-osmotic flow, electrical forces and liquid-liquid interfaces. Barry *et. al.* [5] presented a numerical model for electrokinetic flow of multiphase systems with deformable interfaces based on a combination of the level set and volume of fluid techniques. The presence of electrolyte solutions may cause the drop interface to carry charge. Davidson *et. al.* [6] used an adapted method for capturing interface boundary conditions proposed by Liu *et. al.* [7] to extend the previous numerical model to account for the effect of interfacial charges. This extension allows to analyze the effect of the electrokinetic forces on the deformation of a charged drop in an electrolyte solution.

This research project studies the special case of a cylindrical microchannel with positively charged walls where a perfect dielectric drop with a charged surface is placed inside an electrolyte. The solution and drop flow is driven by an applied electric field. When either the channel walls or the drop interface are charged, electro kinetic phenomena is developed in the microchannel. These phenomena generates charge redistribution due to advection, conduction of ions and diffusion and therefore influences the drop deformation in the channel. Viscous and electrical forces act on the drop accounting for its behavior regarding the motion inside the channel and the deformation. The model was predicted using a computational fluid dynamic (CFD) numerical model [5] that was modified to account for charge density at the drop and liquid interface [6].

3 Theoretical Background

3.1 Electrical Double Layer and Electro-osmotic flow

The first concept that needs to be introduced in order to understand the electro kinetic phenomena inside the microchannel is the electrical double layer. When a solid or liquid surface is in contact with an aqueous solution, its electrical static charges attract counter ions in the solution to the region close to the surface to balance the charges [2]. This region, where there is an accumulation of counter ions is called electric double layer (EDL). This double layer is composed of two layers. The compact layer, where the ions are immobile and strongly attached to the surface is the layer closest to the surface. The diffuse layer is where the ions are mobile and the net charge gradually reduces to zero as the distance from the surface gets larger as seen on Figure 1 Electrical double layer. [1]**Error! Reference source not found.**. The boundary between the two layers of the EDL is at the shear plane, where the liquid velocity is zero and the electric potential is called zeta potential and is considered a constant approximation of the surface electric potential in electro kinetic models [2] .
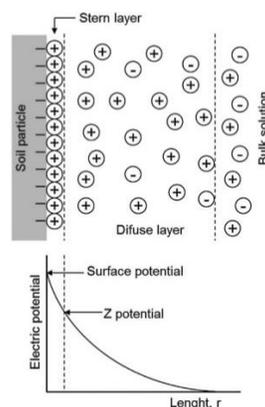

Fig. 1. Electric double layer in a negatively charged soil particle.

Figure 1 Electrical double layer. [1]

The thickness of the EDL is a function of the bulk ionic concentration and electrical proprieties of the liquid and is independent of the solid surface properties [2]. As shown by the equation for the Debye-Huckel parameter, the actual thickness of the EDL is inversely proportional to the bulk ionic concentration. This means that for higher ion concentration, the ions are strongly attracted to the region close to the charged surface, the EDL gets more "compressed" and therefore is thinner.

When an electric field is applied tangentially to the EDL an electric body force is exerted on the counter ions of the diffuse layer of the EDL. The counter ions start to move pulling the liquid with them. The rest of the liquid moves through the channel by viscous forces. This is known as electro-osmotic flow [2]. As seen in Figure 2, the velocity profile of a fully developed electro-osmotic flow is very peculiar and different to the parabolic profile found on viscous flow. In this case, the velocity is zero on the surface, it increases within the EDL, reaches a maximum and becomes a constant in the bulk solution.
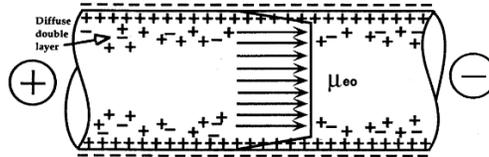

Figure 2 Electro-osmotic flow.

3.2   Governing equations and dimensionless groups

The LS-VOF-based numerical method uses the following equations to describe fluid behavior in the microchannel [8]:

$$\frac{\partial \emptyset}{\partial t} + \nabla.(v.\emptyset) = 0 \tag{1}$$

$$\nabla v = 0 \tag{2}$$

$$\frac{\partial \rho v}{\partial t} + \nabla(\rho vv) = -\nabla p + \frac{1}{Re}\nabla\tau + \frac{1}{We}\delta s f_s + \frac{Ca_E}{We}.\nabla\tau_m \tag{3}$$

5

$$\tau_m = \epsilon EE - \frac{1}{2}\epsilon.(E.E)I \tag{4}$$

Equations 1 and 2 describe the fluid flow in terms of the velocity **v** and the discrete phase volume function **ø**. Equation 3 is the momentum equation, where the velocity is in terms of pressure **p**, the viscous stress tensor **τ** and two additional terms that account for surface force due to interfacial tension (**fs** = surface force and **δs** = delta function for interfacial tension) and electric force via Maxell stress tensor **τm** (Equation 4). **P** and **ε** are fluid density and permittivity, respectively and gravitational terms are omitted for being irrelevant for the momentum in microscale.

$$E = -\nabla U \tag{5}$$

$$\nabla(\epsilon.E) = \rho_e = \frac{1}{2}\kappa^2(n_+ - n_-) + S_q \tag{6}$$

Equations 5 and 6 represent the electric field **E** and the Poisson equation, respectively. While the first one is a function of the electric potential **U,** the second one brings on its right side the dimensionless charge per unit volume due to free ions **ρe** and on the left side the charge per unit volume due to interface charge density q, **Sq**.

$$\frac{\partial ø n_\pm}{\partial t} + \nabla\left(ø n \pm \left(v \pm \frac{1}{Pe}E\right)\right) = \frac{1}{Pe}\nabla(ø\nabla n \pm) \tag{7}$$

Equation 7 describes the ion transport equation, which incorporates advection, diffusion and conduction of ions. **n+** and **n-** are the cations and anions concentrations in the electrolyte solution, respectively Davidson *et. al.* [8].

To account for interfacial charges, two methods were evaluated by Davidson *et. al.[6],* which are the delta function formulation and another one adapted from Liu *et. al. [7]* that accounts for jump in electric displacement due to interfacial charges and discontinuity in permittivity across

interface. Davidson *et. al.[6]* concluded that the second one was more satisfactory to represent the electrical potential jump in the interface. Explicit expressions and formulations for the method can be found in [6, 7].

All the physical variables are nondimensionalized using reference values, giving dimensionless channel and drop radio R and r, respectively, electric field E, permittivity ϵ, surface tension Υ, density ρ and viscosity μ. The time scale t, the velocity V and the free ions concentration n+ and n- were also nondimensionalized. The relevant dimensionless groups seen on the governing equations are as follow:

$$Re = \frac{\rho_{ref} V R}{\mu_{ref}} \qquad We = \frac{\rho_{ref} V^2 R}{\gamma_{ref}} \qquad Ca_E = \frac{\epsilon_0 \epsilon_{ref} E_{ref}^2 R}{\gamma}$$

$$Pe = \frac{VR}{D_{ref}} \qquad \kappa = \left[\frac{2z^2 e^2 n_0 R^2}{\epsilon_0 \epsilon_{ref} kT}\right]^{1/2}$$

Where Re is the Reynolds number, We is the Weber number, Ca_E is the electric capillary number, Pe is the Péclet number and κ is the inverse Debye length. ϵ_0, D, e, z, k and T are respectively the permittivity of free space, diffusivity, the elementary charge, the valence, Boltzmann constant and absolute temperature.

3.3 Numerical model formulation

The numerical model presented by Berry *et. al.* [5] is used for electrokinetic flow of multiphase systems with deformable surfaces. Described in details by Rudman [9], this method is based on a level set-volume of fluid algorithm and features a multiphase formulation of the ion transport equation that accounts for advection, diffusion and conduction of charge carriers within each phase. The electric force present in the momentum equation is accounted for by the Maxwell electric force. A modification on the Nernst-Planck equation for ion transport was made to implement an ion-impenetrable boundary condition and ensure that there would be no ion flux across the interface. The calculation is performed in a two-dimensional axisymmetric staggered grid and the algorithm is an explicit time stepping method with time steps defined dynamically to satisfy stability limits [8].

The presence of charged interfaces causes an associated jump in the electric displacement which was not accounted for in the initial numerical method. Recently, Davidson *et. al.* [6] extended the method to account for surface charge. The new algorithm was based on a method developed by Liu *et. al.* [7] that incorporates jump conditions across surfaces. The electric field is solved in the Poisson equation (6) with a representation of the surface charge S_q. Detailed expressions for the method can be seen in [6-8].

Previous works using this numerical method have shown that a grid resolution of 32 cells is necessary to accurately predict the drop shape [10], therefore this resolution was used in this work. However, a grid refinement showed that a grid resolution of 64 cells could cause a variation of drop velocity of approximately 10%, showing that this could be a potential limitation to the prediction of drop behavior.

4   Literature Review

4.1   Electro-osmotic flow history and applications

The electrokinetic phenomena was first observed by Reuss in 1809, when he observed that water moved through soil pores when an electric potential was applied [3, 11, 12]. In the mid and late 1900 this effect was more widely studied and applied in fields such as drug delivery, chemical analysis [3] and soil stabilization [11]. Over the past years, these phenomena have been widely studied by researchers and applied in many engineering and analytical fields. A variety of numerical methods have been developed to predict electrokinetic and electrohydrodynamic problems especially in nanofluidic and microfluidic, colloid and interface science, analytical chemistry and biochemistry. These models are usually based on combinations of the Navier-Stokes equation for fluid flow and the Poisson-Boltzmann equation for electric potential distribution [12]. Amongst the applications of electro-osmotic flow are electrokinetic treatment of contaminated soil [1, 11], electro-osmotic pumps [3, 12], flow mixing in microchannel [13] and electric field-driven microreactor [14].

The removal of heavy metal contaminants from soils through conventional technologies is extremely hard and the electrokinetic models come as good alternative to this procedure. Experimental [1, 11] as well as numerical models [15] have been developed to describe the efficiency of transportation of ions in soil pores using electric field-driven flows. It was found that chemical nature of soil particles, ionic concentration and ionic strength of inertial fluids, pH, temperature and electrochemical reactions can influence the development and maintenance of electro-osmotic flow [1].

Electro-osmotic pumping have been found to be more effective and advantageous on micro-porous systems than pressure driven mechanisms alone [12]. A few of the primary advantages of this application are the absence of mechanical moving parts of the pump, the possibility to instantly switch flow directions and the capability of generating constant pulse free flows [3].

An active alternative to enhance fluid mixing efficiency is to introduce an external energy source to the mixer and one way of doing it is by applying an electric field to generate electro-osmotic flow [13]. In addition to increasing the flow, this method can also generate vortexes and generate turbulence for a chaotic mixing. Peng & Li [13] studied the influence of ionic concentration on electro-osmotic flow mixing and the dependence of zeta potential, dielectric constant and electric conductivity from this parameter. It was found that for sufficiently high ionic concentrations (Higher than 1M for their case study) resulted in extremely low electro-osmotic flow mobility and non-uniform electric field and velocity flows. Similar results were also found on this research project.

Regarding microreactor, electric field controlled surfaces can have an effect on adsorption and desorption processes relevant to heterogeneous catalysts, when these are in contact with electrolyte solutions [14].

Studies have found that pressure-driven flows through microchannels are influenced by electrokinetic effects [16]. When pressure-driven fluids contain ions and/or microchannels are electrically charged, hydrodynamic resistance can increase due to a flow-induced electric field resulting from streaming potential, so called electroviscous effect [16].

4.2   Liquid droplets inside microchannels

The manipulation of liquid droplets inside microchannels is an important part of the electrokinetic phenomena. It is present in colloid and emulsion industries, especially in nanofluidic and microfluidic. Some potential applications are microcapsules, microreactors, micromixers, lab-on-a-chip and emulsion electrokinetic chromatography (EKC) [4]. The movement of a charged particle relative to a surrounding fluid in response to an applied electric field is called electrophoresis. The principles and equations that describe this phenomena are the same as the electro-osmotic flow [2] and this method is believed to have a great potential in the manipulation of droplets [4].

Lac & Sherwood [17] predicted the influence of a suspended drop in the generation of streaming potential in capillary pressure-driven flow. It was found that the presence of a non-conduction drop can increase the streaming potential by decreasing the average conductivity of the capillary but it can also decrease the streaming potential when it has a lower viscosity than the surrounding fluid, which reduces the pressure difference and hence the streaming current. In this study, the drop surface charge was neglected, which makes it inappropriate for the case of a conducting drop [17].

Furthermore, the motion of a liquid droplet in a cylindrical pore was studied by Huang & Lee [4] with an arbitrary surface potential and electric double layer thickness. A vortex flow was observed due to electric driving force and it was found that a charged wall with opposite sign enhanced drop mobility while same signal charge deterred it [4]. Similar results were also found in this research project, however, different boundary conditions led to divergent conclusions regarding the effect of the electric double layer (EDL) thickness on drop mobility. While Huang & Lee [4] defended that thicker EDL lead to a weaker electro-osmotic flow for having lesser ions per unit volume, this research found that a thicker electric double layer actually enhanced drop mobility. This can be due to the fact that despite having less ions, a thicker electric double layer actually has a greater contact area with the drop and therefore generates more electro-osmotic flow. In addition, Peng & Li [13] studied the effect of ionic concentration on electro-osmotic flow mixing and discovered that higher concentration of ions led to lower electro-osmotic flow, which is consistent with the results presented in this report.

When one of the fluids inside the microchannel (drop fluid or continuous media) is an electrolyte, the drop can also have a deformable surface. This happens because electric forces act on the surface of the drop in opposition to the surface tension. These forces are caused by charge distribution in the electrolyte solution or permittivity jump across the interface, when fluids with different permittivity are contacted. They are also influenced by the presence of electric field in the microchannel. Pillai *et. al.* [10] numerically investigated the deformation and breakup of conducting drops in non-conducting media subjected to an external electric field. The presence of free charges inside the drop created opposing conductive and diffusive fluxes for cations and anions which led to complex ion behavior inside the drop causing its deformation and eventually breakup. This research project investigated the case of a non-conduction drop in a conducting media, which could be the case of an oil drop in water and less drastic drop deformation was observed when compared to [10].

The presence of an electrolyte solution in the microchannel also causes the liquid/liquid interface to carry electric charges due to the adsorption of ions to the surface. The electrokinetic flow model for multiphase flow extended to account for interfacial charges presented by Davidson *et. al.* [5, 6] allows for a better prediction of drop mobility and deformation as well as a comprehensive study of the electrokinetic forces acting on the surface of the drop. This model has recently been validated using analytical solutions and experimental results from published literature [8] and were shown to have accurate predictions. The advances presented by the authors in electrokinetic numerical modeling of microfluidic systems represent an important step towards understanding liquid droplet behaviors in microchannels which is crucial to successful design and operation of numerous applications.

5 Methodology

5.1 Initial conditions

In this project, specific cases were considered with constant dimensionless parameters. A cylindrical microchannel with dimensionless length 14 and radius 1 was considered to be filled with an electrolyte solution and a perfect dielectric drop was placed in the center. The flow was driven by a downwards electric field E = 10 and adjusted to Reynolds = 0.01. The permittivity ratio between the drop and the continuous solution was ϵ_d/ϵ_c = 0.025, the dimensionless density and viscosity of the drop and continuous solution were adjusted to ρ_d = ρ_c = 1 and μ_d = μ_c =1 respectively.

Debye-Huckel parameters of κ = 2 and κ = 8 were considered. For each κ the surface wall was charged with increasing charge densities: S_w = 0, S_w = 4, S_w = 8 and S_w = 16. For each of these cases, the drop interface was either positively or negatively charged, with fix surface charge density S_i = +8 and S_i = -8, respectively, or uncharged, S_i = 0.
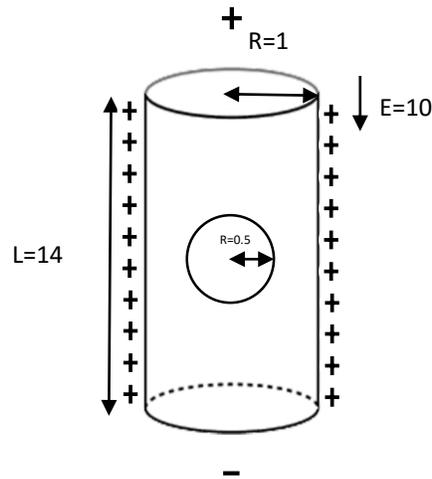

Figure 3 Problem set up: Cylindrical microchannel of radius 1, length 14 and positively charged walls. The flow is driven by a downwards electric field of magnitude 10 and a perfect dielectric drop of radius 0.5 is placed on the central axis of the channel.

5.2   Case study 1: Perfectly spherical drop

In order to study the influence of wall and drop surface charge densities and the thickness of the EDL on the motion of the drop, the Weber number was set to We = 0.001, sufficiently low enough to give a perfectly spherical drop at steady state due to the high surface tension associated with a low Weber number. At steady state, the electro-osmotic flow of the solution, drop velocity, electric field and charge distribution were analyzed.

5.3   Case study 2: Drop with deformation

In the second case study, the surface tension of the drop was decreased to account for drop deformation. While all the other parameters were kept constant and equal to the case study one, the Weber number was increased to We = 0.008, as this parameter is inversely proportional to the surface tension.   The steady state drop deformation, velocity, electric field and charge distribution were analyzed.

5.3.1   Deformation with no permittivity gradient

One of the factors that contribute to the deformation of the drop is the permittivity jump between the drop and the continuous solution, which causes a permittivity force to act on the drop surface. To investigate the relevance of this parameter to drop deformation, the cases of κ = 8, S_w = 8 and S_i = -8, +8 and 0 were investigated with no permittivity jump, or ϵ_d/ϵ_c =1. The charge distribution in a dynamic state were investigated.

6 Results and discussion

6.1 Case study 1: Perfectly spherical drop

6.1.1 Effect of wall and drop surface charge densities on drop velocity

When the external electric field was applied through the channel, the electrical forces acting on the free ions from the electric double layer caused the fluid to move upwards in an electro-osmotic flow. Consequently, the drop was carried along in the same direction. However, if the surface of the drop was charged, an electric double layer was also formed around the drop and the electrical forces acting due to these free ions either enhanced or decreased the drop movement relative to the fluid. Table 1 and Table 2 show the dimensionless velocity of the drop for the proposed cases. The negative velocities for the cases where there was no wall charge and the drop surface was positively charged showed that when there was no electric double layer near the charge driving the fluid upwards, the electrical force surrounding the drop was sufficient to drag it down towards the anode.

Table 1 Dimensionless drop velocity at steady state for We = 0.001 and κ = 2

κ = 2		Wall charge density S_w			
		0	4	8	16
Interface charge density S_i	-8	0.116	0.724	1.06	1.50
	0	0.00	0.551	0.899	1.36
	8	-0.076	0.451	0.799	1.25

Table 2 Dimensionless drop velocity at steady state for We = 0.001 and κ = 8

κ =8		Wall charge density S_w			
		0	4	8	16
Interface charge density S_i	-8	0.0434	0.299	0.531	0.917
	0	0.00	0.241	0.468	0.849
	8	-0.051	0.195	0.415	0.802

From the results shown in the tables above, it was evident that for a higher κ, in other words a thinner electrical double layer, the magnitude of the velocity of the drop was generally smaller. A possible explanation to this is that for a higher κ, the ion concentration in the bulk solution is higher which causes the free ions in the diffuse layer of the electrical double layer to be more 'compacted' and closer to the charged surface. In addition to the compaction, the area in which the ions move to create the flow is smaller, therefore a weaker electro-osmotic flow is generated. Since we only tested two values of κ, it is not possible to conclude that this is always the case. In fact, [4] studied a similar case with a spherical drop with an electro-osmotic flow in a microchannel and the drop mobility as a function of κ was shown to vary significantly when other parameters were altered. It either increased or decreased depending on the range of κ and other factors such as viscosity ratio, drop to channel ratio and the zeta potential. On the other hand, when studying electrolyte fluid mixing in a microchannel Pang & Li [13] found that higher ionic concentrations gave lower electro-osmotic flow mobility.

Regardless of the drop interface charge density, the higher the wall charge density, the faster the fluid, and consequently the drop, moved. This was due to the fact that for a given ionic concentration in the bulk solution (a given EDL thickness), higher charge density attracted more counter ions to the EDL and therefore a stronger electric force resulted in a higher velocity.

When compared to the uncharged drop surface of same κ and same wall charge density, the negatively charged drop moved faster and the positively charged drop moved slower. Since the electric field was applied downwards and the channel walls were positively charged, the EDL near the wall had an excess of negative ions that caused the fluid to move upwards in the direction of the cathode. The negative charges on the drop surface also tended to move towards the positive end of the channel, and therefore the velocity of the drop was enhanced. Similarly, the positive charge density on the drop surface would tend to move away from the positive end of the channel and therefore the overall drop velocity was decreased. This result was consistent to that presented by [4] as it was found that for a given κ, a positively charged wall slowed a positively charged drop down and a negatively charged wall enhanced its velocity. In conclusion, the drop velocity will be enhanced when drop surface and wall have opposite charges and it will be decreased when they have the same charge.

6.1.2 Electro-osmotic flow and vortex flow

The velocity profile of the fluid inside the channel was consistent to what is expected in an electro-osmotic flow, especially for a thinner electric double layer, as shown in Figure 4 a) and b). The velocity was zero on the surface and increased significantly along the diffuse layer of the electric double layer. For κ = 8 (Figure 4 a) it reached a constant velocity in the bulk solution and showed a plug-flow profile. On the other hand, for κ = 2 Figure 4 b), the electric double layer was too thick compared to the channel radios and therefore, a plug flow is not observed in the bulk solution. The final velocity of the fluid increased proportionally to the wall charge densities. Figure 4 shows the velocity profiles of the fluid inside the channel positioned away from the drop for κ = 8 and κ = 2 whilst increasing the wall charge densities. These results were similar regardless of the drop surface charge density as it is independent of this parameter. It is also evident from Figure 4 that a thicker EDL (smaller κ) generated greater electro-osmotic flow.
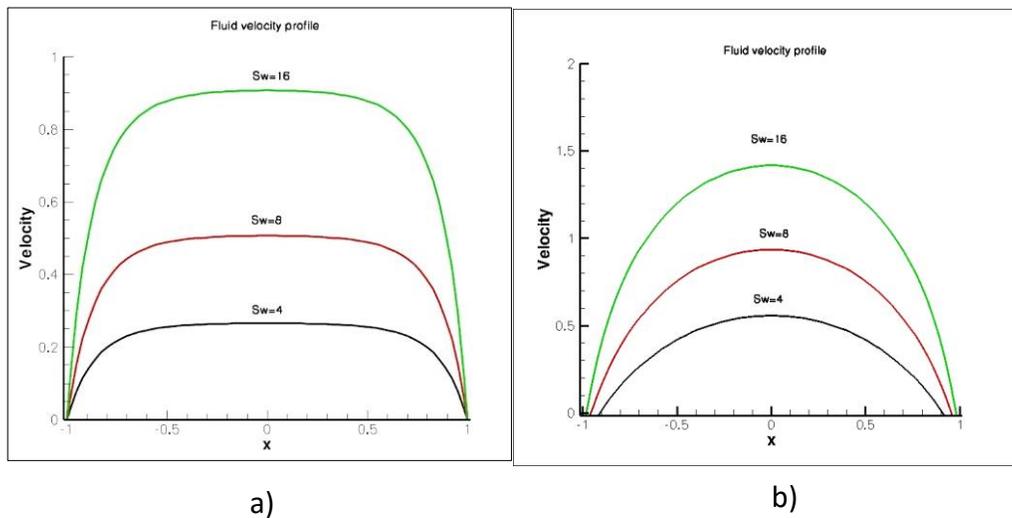

a)

b)

Figure 4 Fluid velocity profile away from the drop for We=0.001, a) κ = 8 and b) κ = 2

An interesting axisymmetric vortex flow was observed inside the droplet when it was positively or negatively charged with different internal flow directions for each charge (Figure 5). Similar results were also observed by [4] and the explanation for this phenomena is the competition between hydrodynamic dragging forces and the electric forces acting on the surface of the drop. Figure 5 a) and b) shows the vectors of the fluid velocity relative to the drop velocity for a particular case. Similar vortexes were found in all the cases studied in this research project.

For the negatively charged drop, the fluid moves slower than the drop, which is evidenced by the downward relative velocity vectors outside the drop on the surrounding fluid. However, the fluid that is immediately adjacent to the drop surfaces on its sides is actually moving faster than the drop. This is explained by the fact that negative charges on the drop surface create an electric field pointing away from the drop. The resulting force due to this electric field acts locally on the adjacent fluid making it move faster. As a result, the fluid inside the drop displays the vortex flow as shown in Figure 5 a).

The exact opposite is observed on the positively charged drop. In the bulk solution, the vectors pointing upwards indicate that the surrounding fluid is moving faster than the drop, which does not occur on the fluid immediately adjacent to the drop surface. The positive charges on the drop surface create an electric field pointing towards the drop. The resulting electrical force in this case acts slowing the adjacent fluid and creates a vortex on the opposite direction to the one observed previously. Figures of the electric field vectors can be seen in Appendix 2.
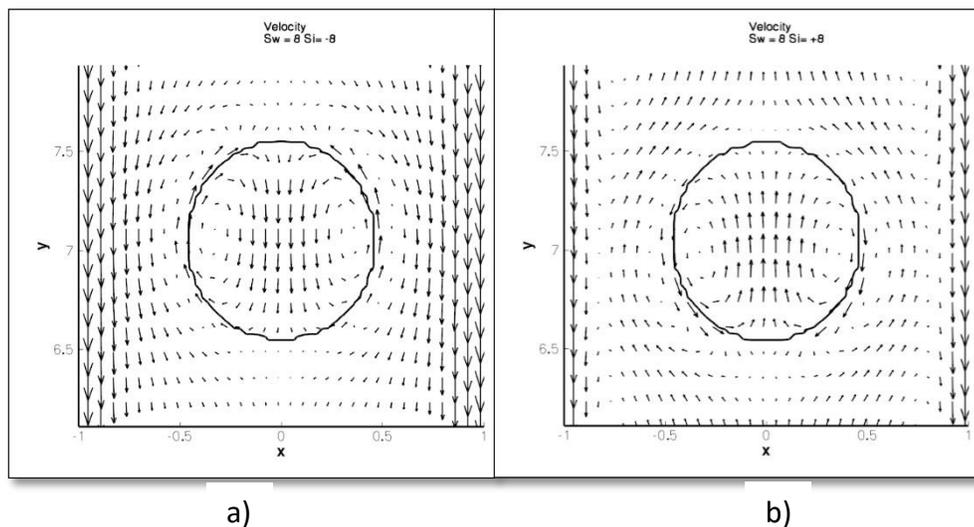

a)   b)

Figure 5 Velocity of the fluid relative to the drop for We = 0.001, κ = 8, Sw = 8 and a) Si = -8 b) Si = +8

Such phenomena is not observed when the drop surface is uncharged as the fluid inside the drop moves at the same velocity of the surrounding fluid. This is due to the absence of sufficient surface charges to create electric field normal to the drop surface. The lack of a strong normal electric field and electric forces acting on the drop surface allow the fluid to be carried along with the solution mainly by viscous forces. The observation of these vortexes generated by electro-

osmotic flow is particularly relevant for the application of chaotic electro-osmotic flow fluid mixing [13], as they can enhance the mixing rates.

6.1.3   Charge distribution and Electric field magnitude

Figure 6 shows the charge distribution in the microchannel for the case where We = 0.001 and the drop is perfectly spherical at steady state. Figure 6 a) and b) give EDL thickness of κ = 8 and κ = 2 respectively, fix wall charge density Sw = 8 and drop surface charge density of Si = -8, 0 and 8.

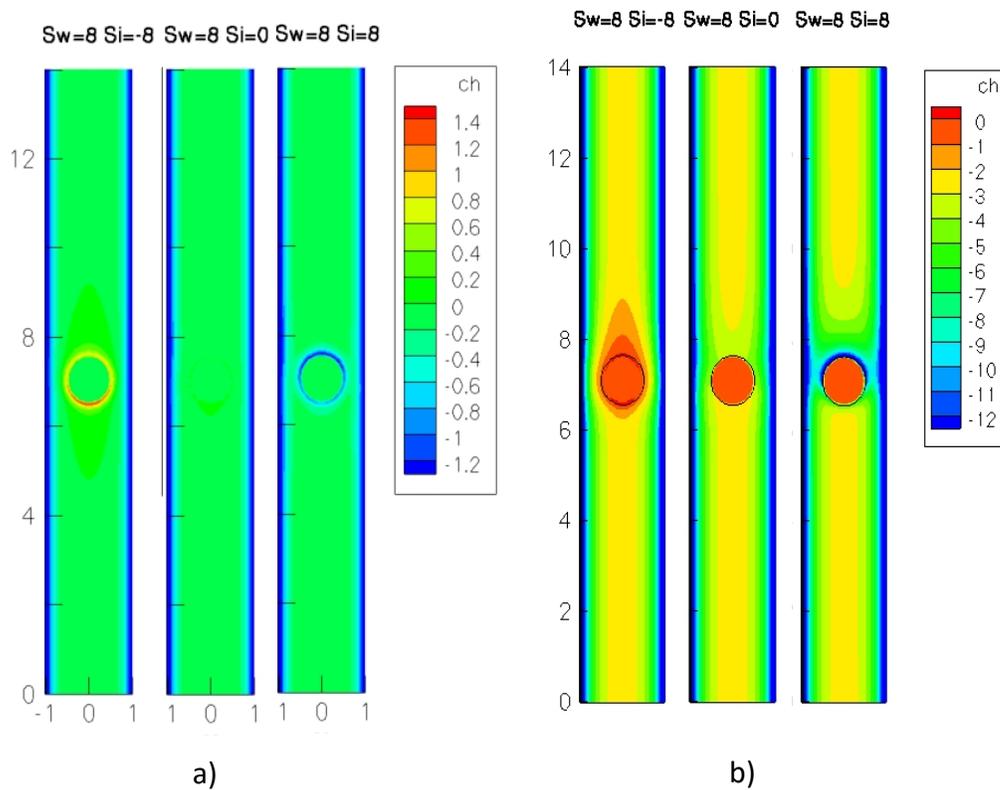*Figure 6 Charge distribution for We = 0.001, a) κ = 8, Sw = 8 and Si = -8, 0 and +8*
b) κ = 2, Sw = 8 and Si = -8, 0 and +8

As seen from figure 6 a), an inverse Debye length parameter of κ = 8 gives a thin EDL. In most part of the microchannel width the charge concentration in the bulk solution is zero. This is consistent with the plug flow profile of the electro-osmotic flow observed for this case (Figure 4 a). On the other hand, Figure 6 b) evidences that for κ = 2, the thickness of the electric double

layer is greater than the radios of the channel and therefore a negative charge accumulation is observed throughout the entire channel. This explains why the plug flow profile was not observed for this case (Figure 4b). Davidson *et. al.* [8] have also shown that in a pressure-driven flow, the choice of $\kappa = 2$ allows the EDL to extend to the centerline of the channel and the charge remains negative.

For both $\kappa = 8$ and $\kappa = 2$, the positively charged drop displayed an accumulation of negative charge around the interface. It can be seen from Figure 6 that the accumulation of negative charges was greater at the top of the drop. This can be explained by looking at the electrolyte solution movement, which is due to bulk convection, the diffusion and ion migration [8]. Although the diffusion component should be uniform around the drop due to the constant charge density, the convection component of the fluid movement will tend to keep the ions at the top, or at least slow down the rate that it is distributed to the lower parts of the drop, since the fluid is moving upwards relative to the drop.

Figure 6 also shows that for $\kappa = 8$ (thinner EDL), the positive charge accumulation around the negatively charged drop was greater at the top. Similarly, the diffusion component should be uniform around the drop due to the constant charge density, but in this case, the convection component of the fluid movement will tend to drag the ions to the bottom of the drop, as the surrounding fluid is moving downwards relative to the drop. As it can be seen from Figure 6 b), the negatively charged drop with $\kappa = 2$ did not have a positive charge accumulation surrounding it. Despite the attraction of positive charges to the region near the drop surface, the magnitude of the negative charges in the bulk solution was high enough to prevent a positive charge distribution. However, the effect of the convection component of the movement is still evident from the shape of the 'less negative' region surrounding the drop. Since the drop is moving slower than the surrounding fluid, the effect on charge distribution was greater at its top.

The magnitude of the total electric field E inside the channel is presented in Figure 7 for the case study of We = 0.001, $\kappa = 8$ and $\kappa = 2$, with wall charge density Sw = 8 and drop interface charge density Si = -8, 0 and 8. This field is a combination of the applied electric field, the electric field due to the free charges in the electric double layer near the wall and the drop surface. It is also

influenced by the difference in permittivity from the drop and the continuous fluid. These effects are evident from the solution of the Poisson equation (6) for the electric field.
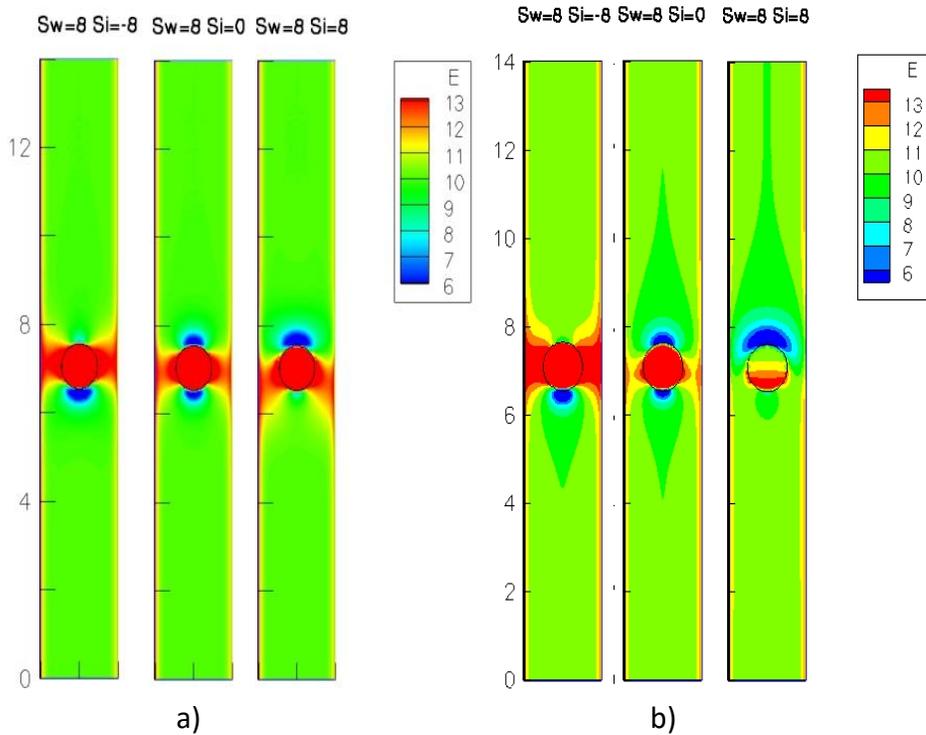

Figure 7 Total Electric Field magnitude for a) We = 0.001, a) κ = 8, Sw = 8 and Si = -8, 0 and +8 b) We = 0.001, κ = 2, Sw = 8 and Si = -8, 0 and +8

For κ = 8 (Figure 7 a), the total electric field is constant in the bulk solution and equal to the applied electric field. Close to the wall, the electric field is greater than 10 due to the overlap of the electric double layers surrounding the drop interface and the wall. It is also observed that there is an enhancement of the total electric field inside the drop, where the fluid has a lower permittivity. This enhancement is also observed on the sides of the drop, which can be explained by the overlapping of electric double layers from both drop and wall charges. Although is not clear for the chosen color scale, the total electric field in the microchannel of κ = 2 (Figure 7 b) is slightly higher than 10, which is caused by the excess of negative charges along the channel.

It can also be seen from Figure 7, for both κ = 8 and κ = 2 that there is a depletion of the total field on the top of the negatively charged drop and at the bottom of the positively charged drop. In the first case, the negative charges from the surface create a field pointing inwards to the drop. At the bottom, this field is upwards and therefore cancels out the applied field decreasing the

overall E. The opposite occurs to the positively charged drop, as it creates an electric field pointing outwards from the drop and at the top it cancels out the applied field decreasing the overall electric field. Although it is not clear from Figure 6, (See Appendix 1) there is a slight negative charge accumulation near the surface of the uncharged drop due to the advection of ions in the electrolyte solution. This accumulation can explain why there is an enhancement of electric field on the sides and a depletion at the top and bottom of the drop. Another possible explanation is the permittivity jump across the interface that also generates an electric field jump.

6.2   Case study 2: Drop with deformation

6.2.1   Effect of wall and drop surface charge densities on drop velocity

The results of the drop velocity at the steady state from case study two are shown on Table 3 and Table 4. Similarly to case study one, the drop velocities were greater for a lower κ and increased as the wall charge density increased. The velocities of the uncharged drops were very close to the velocities from case one and were either enhanced or decreased by the drop surface charge densities depending on its sign. However, the effect of the drop surface charge density was shown to be greater for the case with We = 0.008. This means that the negatively charged drops moved even faster and the positively charged drops moved even slower when compared to the drops of same κ and wall charge density from case study 1. The same vortex flows that occurred on case study one were observed for this case.

Table 3 Dimensionless drop velocity for We = 0.008 and κ = 2

κ=2		Wall charge density S_w			
		0	4	8	16
Interface	-8	0.555	0.923	1.196	1.605
charge	0	0.003	0.556	0.907	1.358
density S_i	8	-0.27873	0.41255	0.75599	1.2127

Table 4 Dimensionless drop velocity for We = 0.008 and κ = 8

κ=8		Wall charge density S_w			
		0	4	8	16
Interface	-8	0.122	0.378	0.608	0.981
charge	0	0.037	0.241	0.468	0.847
density S_i	8	-0.1214	0.150	0.386	0.785

6.2.2   Drop deformation

Figure 8 Drop contour for We = 0.008, a) κ = 8, Sw = 8 and Si = -8, 0 and 8In this case study, the surface tension was decreased in a way that the Weber number was increased to 0.008. The reduction of surface tension allowed for electric forces to act more incisively on the surface of the drop and cause some degree of elongation. Drop elongation when in the presence of charged walls was also found for a pressure-driven flow with similar conditions by Davidson *et. al.* [8]. It was observed that the wall charge density was not relevant to the drop deformation, as the deformation for higher and lower wall charge densities were very similar to the one in Figure 8 for Sw = 8Figure 8 (Results not shown). This is an evidence that the effect of increasing the surface charge density on drop deformation is small when compared to changing the ionic concentration of the bulk solution, defined in this research by the Debye length parameter, κ.
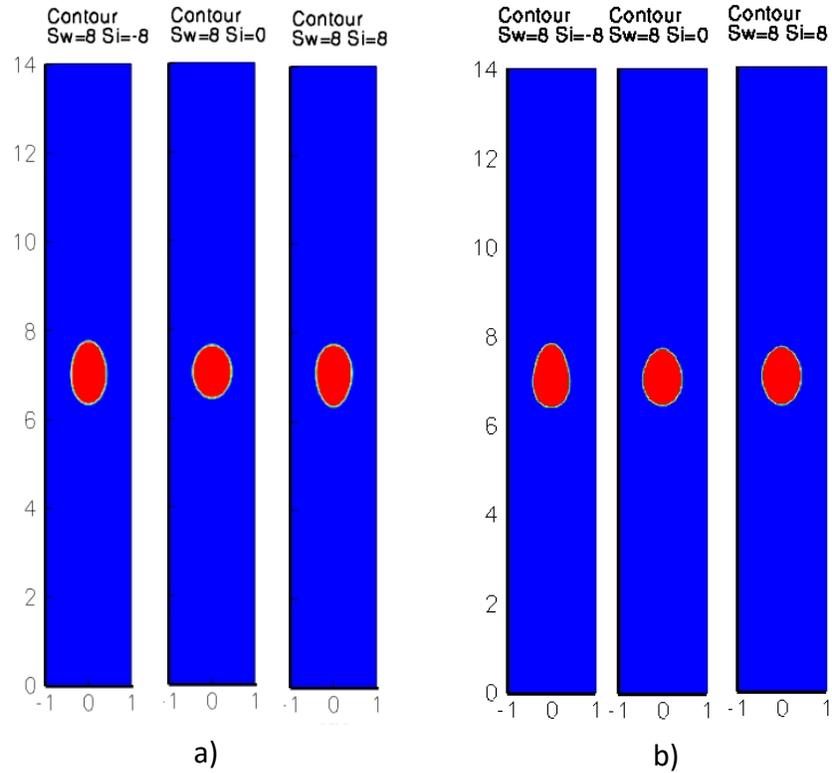
Figure 8 Drop contour for We = 0.008, a) κ = 8, Sw = 8 and Si = -8, 0 and 8
b) κ = 8, Sw = 8 and Si = -8, 0 and 8

It is evident from Figure 8 Drop contour for We = 0.008, a) κ = 8, Sw = 8 and Si = -8, 0 and 8 that the uncharged drop suffered less deformation than the charged ones. This is explained by the smaller effect of the electro kinetic forces due to charge distribution around the drop. For the deformation of the charged drops, three factors are potentially influencing the deformation. The first factor is the hydrodynamic forces from the fluid adjacent to the drop having a more significant impact on the drop shape, due to the lower surface tension of the drop. The second factor is the charge forces that the counter ions distributed around the charged surface of the drop exerted on it. And the third factor is the permittivity force due to the permittivity jump on the surface, given that the permittivity ratio was ϵ_d/ϵ_c = 0.025. These electro kinetic forces are also enhanced by the presence of the applied electric field through the microchannel. A similar inwards lateral force due to permittivity jump in combination with electric field was also found by Davidson *et. al.* [8] for a case with charged walls and charged drop interface.

Comparing the different EDL thickness, it is possible to conclude that for a thinner EDL (Figure 8 a, κ = 8) the deformation of both negatively and positively charged drops were very similar, being influenced mainly by the permittivity jump and the distribution of charges surrounding the drop. For a thicker EDL (Figure 8 b, κ = 2), on the other hand, the deformation of the negatively charged drop was visibly greater than the positively charged drop. This is explained in more details in the next section.

6.2.3   Effect of charge distribution and Electric field on drop deformation

Figure 9 shows the charge distribution in the microchannel for the case where We = 0.008 and the drop experiences some deformation. Figure 6 a) and b) give EDL thickness of κ = 8 and κ = 2 respectively, for fix wall charge density Sw = 8 and drop surface charge density of Si = -8, 0 and 8.
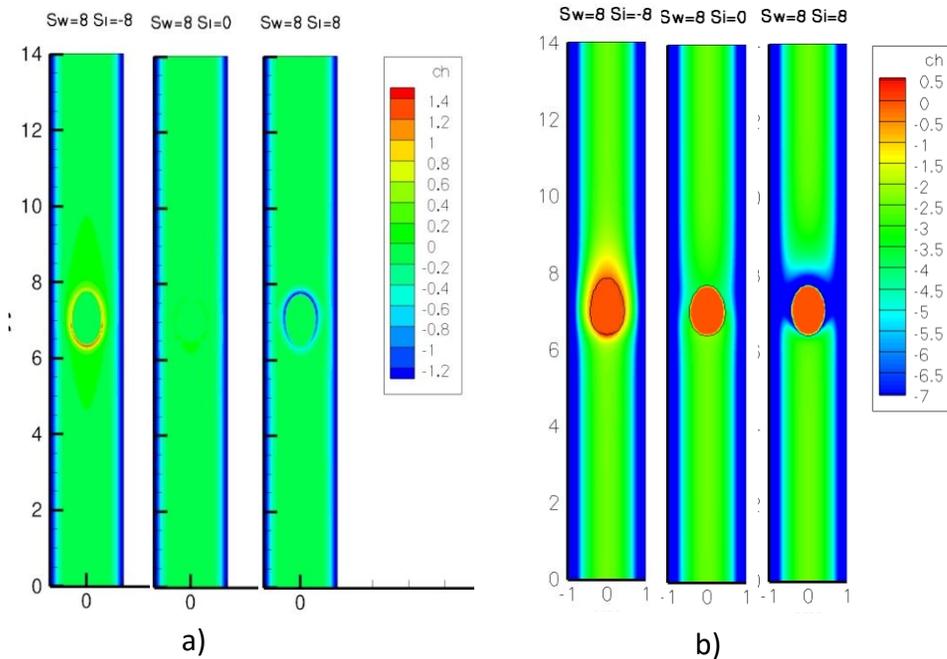

Figure 9 Charge distribution for We = 0.008, a) κ = 8, Sw = 8 and Si = -8, 0 and +8
b) κ = 2, Sw = 8 and Si = -8, 0 and +8

Similarly to case study one, the distribution of charges around the drop was shown to be non-uniform due to hydrodynamic and electrokinetic effects. It is clear from figure 9 a) and b) that the EDL for κ = 8 is very thin when compared to the channel radio and for κ = 2 it extends through

the centerline of the channel leaving it somewhat negative. For κ = 8 (Figure 9 a), the distribution of positive charges around the negatively charged drop was higher at the bottom of the drop while the distribution of negative charges around the positively charges drop was higher at the top. The explanation is equivalent for case study one and was fully explained in section 6.3.1. Furthermore, for κ = 2, the negatively charged drop caused a reduction on the highly negative section of the wall EDL and also decreased the intensity of negative charges accumulation around the drop itself. The positively charged drop, on the other hand, caused this section of the EDL to increase, overlapping the EDL due to the drop surface charges.

The distribution of charges in the microchannel due to charged interfaces in combination with the applied electric field contribute to deformation by applying an electric force (charge force) on the surface of the drop. This effect is combined with the effect of a permittivity force generated by a permittivity jump across the interface (permittivity ratio ϵ_d/ϵ_c = 0.025) and in opposition to the surface tension. Since the surface tension and permittivity factors are the same for all the cases presented in Figure 9, it is clear that the charge effects vary for different drop surface charge and the inverse Debye length parameter, which is related to the EDL thickness and ion concentration in the bulk solution.

For κ = 8 (Figure 9 a), the deformation is similar for both negatively and positively charged drops and greater than the uncharged drop. Moreover, for κ = 2 (Figure 9 b), the charge effects seem to be affecting more the charge deformation. This is somehow expected, since the entire channel contains excess negative charges due to the EDL near the wall. This is possibly the main reason for the uncharged drop being more deformed more than when κ = 8. Furthermore, in this last case, the negatively charged drop deformed more than the positively charged drop.

The magnitude of the total electric field E inside the channel is presented in Figure 9 for the case study of We = 0.008, κ =8 and κ = 2, with wall charge density Sw = 8 and drop interface charge density Si = -8, 0 and 8.
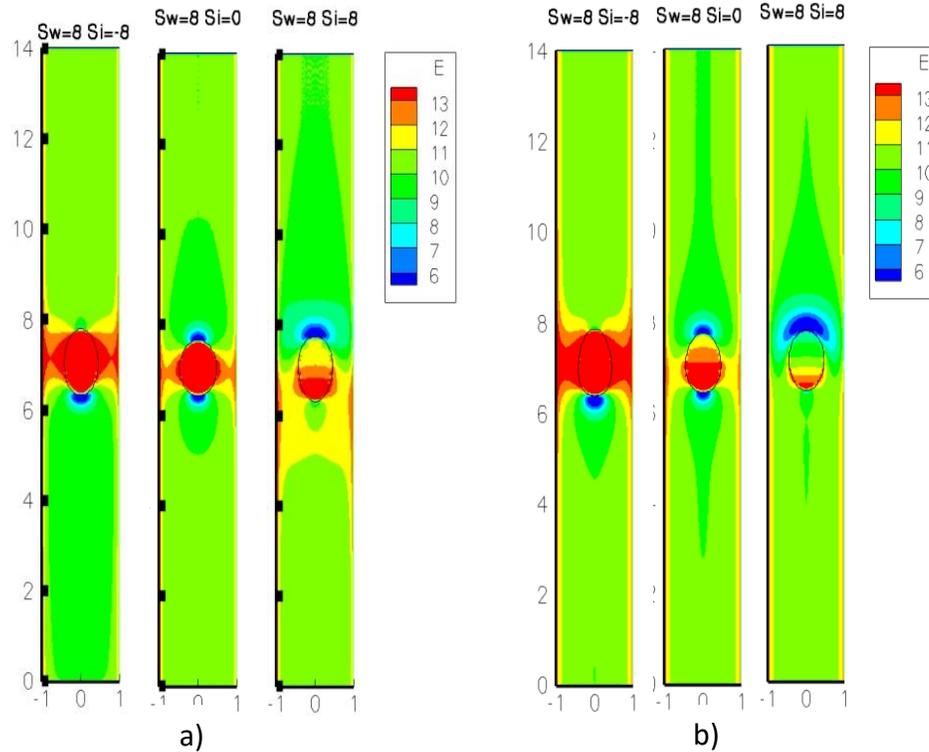
*Figure 10 Total Electric Field magnitude for We = 0.008, a) κ = 8, Sw = 8 and Si = -8, 0 and +8
b) κ = 2, Sw = 8 and Si = -8, 0 and +8*

Similarly to case study one, the distribution of total electric field is influenced by the application of an external electric field as well as that created by the charge distributions along the channel. In figure 10, depletion of the total field was observed on the bottom of negatively charged drops, at the top of positively charged drops and on both top and bottom of uncharged drops. This could be caused by the fact that a permittivity jump across the interface creates a jump in the electric field in the normal direction to the surface. In addition, the electric field created by the drop surface charges are acting normally to the surface in opposite directions resulting in depletion and enhancement patterns observed. Appendix 3 shows electric field vectors for a particular case to exemplify this difference in field directions.

6.2.4 Deformation with no permittivity gradient

It is known that a combination of charge forces and permittivity forces is responsible for the drop deformation but it is unclear what the individual contribution of each force is to the final result. To further investigate the effect of the permittivity force on drop deformation, some cases were ran with no permittivity jump across the drop interface, in other words, both the drop phase and fluid phase had equal permittivity, $\epsilon_d = \epsilon_c = 1$. The cases of We = 0.008, κ = 8, Sw = 8, Si = -8, 0 and 8 were tested and the results are shown in Figure 11:
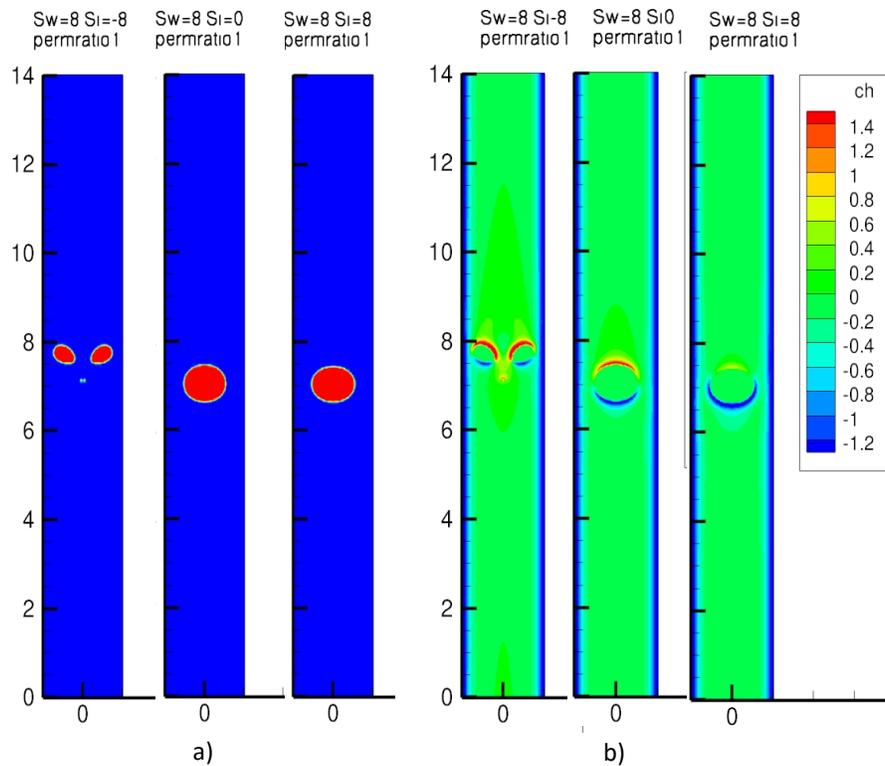

Figure 11 Deformation with no permittivity jump. εd = εc = 1, We = 0.008, κ = 8, Sw = 8, Si = -8, 0 and 8. a) Drop Contour and b) Charge distribution

As seen in figure 11 a), the drop deformed differently when no permittivity jump was present. Instead of being squeezed from the sides and presenting a vertical elongation like the initial case, a horizontal deformation was observed and in some cases broke into two smaller drops from the central vertical axis. The charge distribution shown in Figure 11 b) suggests that the accumulation of charges at the bottom and top of the drop was even more significant in this case. It is believed

that because there were no permittivity forces acting normally to the surface of the drop, the resulting force due to the charge accumulation at the top and bottom of the drops was sufficiently strong to cause the drop to flatten. In addition, the hydrodynamic effects of fluid movement being smaller on the surface could also have contributed to the resulting charge distribution. This effect is more evident on the uncharged drop, where the separation of positive and negative charges was very significant at the top and bottom of the drop.

Moreover, the breakup of the negatively charged drop can be explained by a combination of the charge forces and the movement of the drop. The accumulation of positive charges at the top exerted a force into the drop, causing it to flatten up. Since the drop was moving faster than the surrounding fluid and in an opposite direction to the applied force, this force was enhanced and so was the accumulation of positive charges at the top. As the positive charge accumulated, the electric force due to the charge increased even further, resulting in a positive "valley" at the top of the drop causing its breakup. Figure 12 shows the charge distribution at different dimensionless time steps before reaching steady state, supporting the explanation given above.
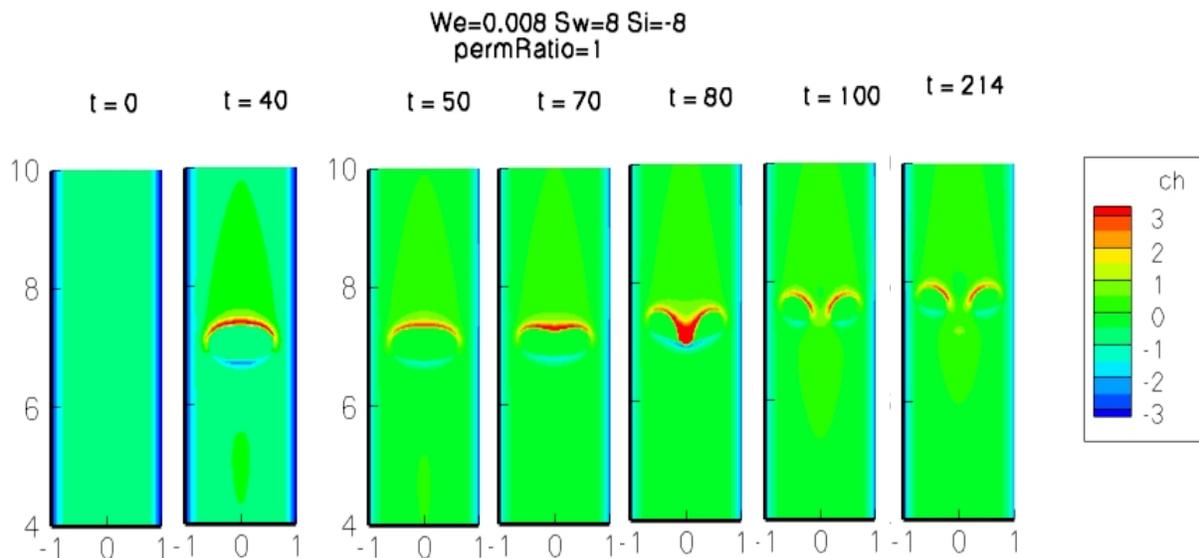

Figure 12 Deformation with no permittivity jump. Charge distribution in dynamic time steps. $\epsilon_d = \epsilon_c = 1$, We = 0.008, $\kappa = 8$, Sw = 8 and Si = -8, 0 and +8 = 8, Sw = 8, Si = -8.

Initially, there was no charge accumulation and it increased with time. The initial time steps from t=0 to t=40 have very small charge variations, therefore it was used a charge scale of -1.5 to 2 (not shown in Figure 12).

Similar behavior was no seen in the positively charged drop. This one had an accumulation of negative charges at the bottom. Hence, its deformation was due to charge forces applied from the bottom up. The forces applied on the positively charge drop were on the same direction as the fluid motion and therefore the charge forces were not sufficient to cause drop breakup.

7   Conclusions

The motion and deformation of a perfect dielectric drop inside a microchannel filled with an electrolyte solution under electric-driven flow were investigated numerically using a computational dynamic fluid model proposed by Davidson *et. al.* [5] and extended to account for the presence of charged liquid/liquid interfaces [6]. Electrokinetic effects such as charge distribution, electric field magnitude and electric double layer thickness on drop mobility and deformation were analyzed. A cylindrical microchannel with fixed dimensionless parameters was used with arbitrary inverse Debye length parameter κ = 8 and κ =2. The wall was positively charged with increasing surface charge densities (Sw = 0, 4, 8 and 16) and the drop surface was either uncharged, positively or negatively charged (Si =0, -8, or 8). All these cases were divided into two major case studies: the first with We = 0.001 giving a spherical drop at steady state and the second with We = 0.008 which allowed for drop deformation.

In the first case study (We = 0.001), the spherical drop was moving upwards due to electro-osmotic fluid flow caused by the application of the electric field. The drop velocity was generally higher for a lower κ, which can be explained by a greater area of electro-osmotic flow induction due to a thicker EDL. The wall charge density was found to influence the drop and fluid velocities as the velocity increased for higher wall charge density. With regards to the drop charge density, the drop velocity was enhanced when drop surface and wall had negative and positive charges, respectively and decreased when both had positive charges. This was expected, since the

negative charges on the drop surface as well as the negative counter ions of the EDL would tend to move towards the positive electrode while the positive charges on the drop surface would tend to move away from it, hence slowing the drop down.

For κ = 8, the EDL was thin compared to the channel radio which was proven by the plug flow velocity profile inside the channel and the charge distribution being neutral inside. For κ = 2, on the other hand, the EDL was found to be thick enough to extend to the centerline leaving a somewhat negative channel and no plug flow was observed. An interesting axisymmetric vortex flow was observed inside the droplet when it was positively or negatively charged with different internal flow directions for each charge. This phenomena was due to the competition between hydrodynamic dragging forces and electric forces acting on the surface of the drop.

The charge distribution around the drop was found to be non-uniform due to electrokinetic and hydrodynamic effects on the electrolyte transportation mechanism. There was a greater accumulation of positive charges at the bottom of negatively charged drop and of negative charges at the top of the positively charged drop. This is caused partially by the convection effect of ion transportation and enhanced by the relative velocity of the fluid to the drop being opposite in both cases. The distribution of the total electric field was also non-uniform inside the channel. It was a combination of the applied electric field, the electric field generated by the EDL and the permittivity difference across the drop interface.

 In the second case study, the velocity of the uncharged drops remained almost equal to the case study one and the effect of drop charge density in the enhancement or depletion of drop mobility was even bigger, with the negatively charged drops moving faster and the positively charged drops moving slower than in case one. Vortex flows inside the drop were also observed. The deformation suffered from the drop was an elongation in the central axis. Charged drops deformed more than uncharged drops, for κ = 8 positively and negatively charged drops deformed equally and for κ = 2 the negatively charged drop deformed more than the positively charged one, which is still to be explained. However, it is known that the deformation is caused by a combination of charge forces as well as permittivity forces acting on the drop surface. Hence, the influence of the permittivity force was investigated by comparing the results with a case with

no permittivity jump across the interface. This case presented a horizontal deformation due to the charge accumulations at the top and bottom of the drop. This evidences that the permittivity force was responsible for squeezing the drop from the sides and creating the elongation.

The understanding of drop behavior and electrokinetic effects in microfluidic systems is extremely important for numerous applications. This study was an example of the contribution of a new numerical model and how it can be applied to better predict these systems and hence help the design and operation of new technologies.

8 Suggestion for further work

The numerical model formulation presented in this study was recently extended to account for liquid-liquid surface charges, which is a significant improvement to the simulations regarding the modelling of droplet motion and deformation in microchannels. Since then, it has been applied to problems involving drop deformation and breakup [10] and compared to analytical solutions for drop relaxation in the presence of ion and interfacial charge and shape evolution of a critically charged water droplet in air [8]. To further comprehend the effects of these charged surfaces it would be interesting to simulate previously studied cases, such as the electrophoretic motion of a liquid droplet in a cylindrical pore [4] to compare previous results and investigate its relevance to this particular study. The effect of fixing the thickness of the electric double layer by fixing the Debye-Huckel parameter on the drop mobility is still unclear and should be given further consideration. A grid refinement to 64 cells resolution showed a variation in drop velocity of approximately 10%, showing that the current resolution of 32 mesh could have limitations on predicting drop behavior. Hence, a further study with a more refined mesh resolution would be necessary to determine the validity of these results.

The addition of surfactant or emulsifiers to solutions containing droplets can significantly reduce its surface tension [18]. Hence, by analyzing real systems with large Weber numbers, and therefore low surface tensions, will be useful to measure the strength of the electrical forces

acting on the drop deformation and breakup in nature. This study only considered drops with constant charge density, but depending on the system, the total charge can be fixed and the charge density can vary as the drop deforms and change its surface area. Therefore, using this numerical model with an initial condition set up to such that the total surface charge is constant instead of surface charge density is also a subject of interest. Lastly, a fixed charge density of $S_i=\pm8$ was considered, which is below the critical stability. But, as the surface charge increases, the drop can eventually reach a critical Rayleigh instability value and break up due to electrical repulsion forces within the surface charges.

9 Appendix

Appendix 1 – Charge distribution around the uncharged drop for κ = 8 (Comparison with the larger range scale for the charged drops) and κ = 2. For the latest there was almost no charge distribution around the drop.
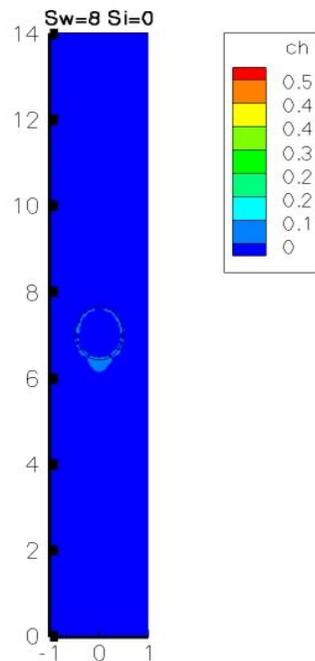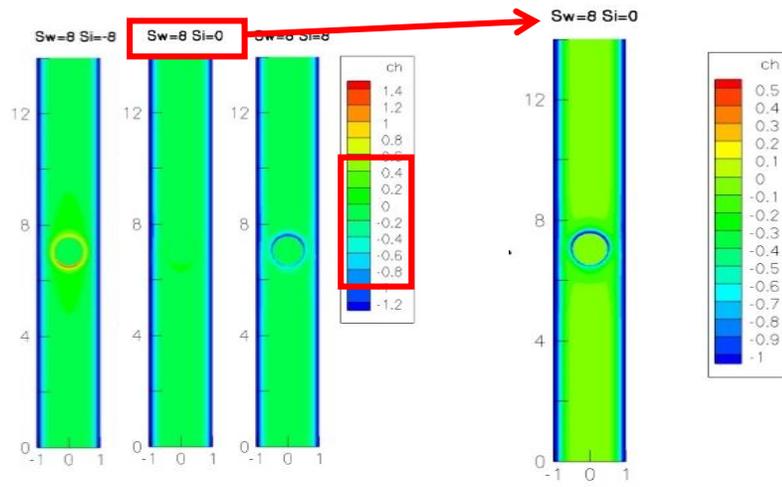
Appendix 2 –Electric field vectors for the case of We = 0.008, κ = 8, Sw = 8 and Si = -8, 0 and 8.
For a negatively charged drop, a field pointing away from the drop is created while for the
positively charged drop the field created is pointing inwards to the drop. This effect is minimized
by the combination with the applied electric field.
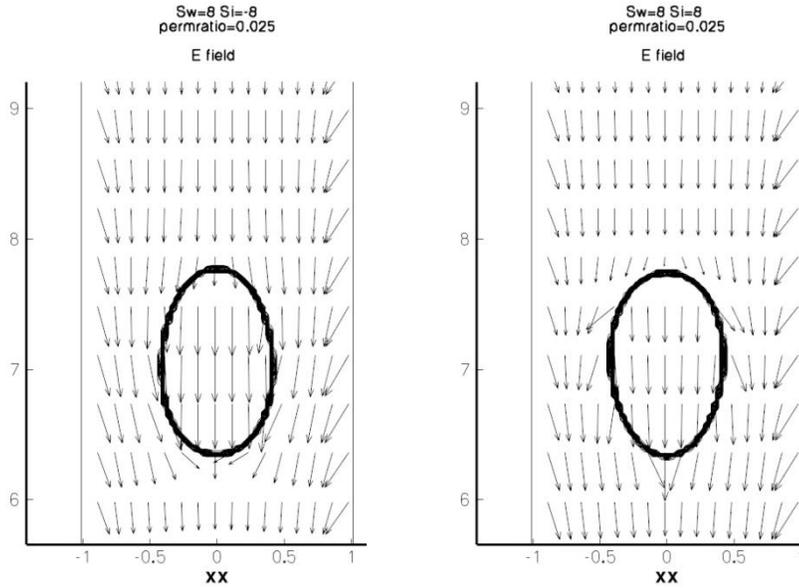
10 References

1. Cameselle, C., *Enhancement Of Electro-Osmotic Flow During The Electrokinetic Treatment Of A Contaminated Soil.* Electrochimica Acta, 2015. **181**: p. 31-38.
2. Li, D., *Electrokinetics in Microfluidics*. 2004.
3. Wang, X., et al., *Electroosmotic pumps for microflow analysis.* TrAC Trends in Analytical Chemistry, 2009. **28**(1): p. 64-74.
4. Huang, C.-H. and E. Lee, *Electrophoretic Motion of a Liquid Droplet in a Cylindrical Pore.* The Journal of Physical Chemistry C, 2012. **116**(28): p. 15058-15067.
5. Berry, J.D.D., Malcolm R.; Harvie, Dalton J. E., *A multiphase electrokinetic flow model for electrolytes with liquid/liquid interfaces.* Journal of Computational Physics, 2013. **251**: p. 209-222.
6. Davidson, M.R.B., Joseph D.; Harvie, Dalton J. E., *Numerical simulation of the deformation of charged drops of electrolyte.* Advances in Fluid Mechanics X, 2014.
7. Liu, X.-D., R.P. Fedkiw, and M. кang, *A Boundary Condition Capturing Method for Poisson's Equation on Irregular Domains.* Journal of Computational Physics, 2000. **160**(1): p. 151-178.
8. Davidson, M.R., et al., *Numerical simulation of two-fluid flow of electrolyte solution with charged deforming interfaces.* Applied Mathematical Modelling, 2015.
9. Rudman, M., *A volume-tracking method for incompressible multifluid flows with large density variations.* International Journal for Numerical Methods in Fluids, 1998. **28**(2): p. 357-378.
10. Pillai, R., et al., *Electrolytic drops in an electric field: A numerical study of drop deformation and breakup.* Physical Review E, 2015. **92**(1): p. 013007.
11. Sahoo, S., B.R. Paramkusam, and R. Srivastava, *DEVELOPMENT OF A MODEL FOR ELECTRO кINETIC STUDY.*
12. Li, B., et al., *Evaluation of electro-osmotic pumping effect on microporous media flow.* Applied Thermal Engineering, 2013. **60**(1–2): p. 449-455.
13. Peng, R. and D. Li, *Effects of ionic concentration gradient on electroosmotic flow mixing in a microchannel.* Journal of Colloid and Interface Science, 2015. **440**: p. 126-132.
14. Susarrey-Arce, A., et al., *A new ATR-IR microreactor to study electric field-driven processes.* Sensors and Actuators B: Chemical, 2015. **220**: p. 13-21.
15. Gomes, H.I., et al., *Numerical prediction of diffusion and electric field-induced iron nanoparticle transport.* Electrochimica Acta, 2015. **181**: p. 5-12.
16. Davidson, M.R. and D.J.E. Harvie, *Electroviscous effects in low Reynolds number liquid flow through a slit-like microfluidic contraction.* Chemical Engineering Science, 2007. **62**(16): p. 4229-4240.
17. Lac, E. and J.D. Sherwood, *Streaming potential generated by a drop moving along the centreline of a capillary.* Journal of Fluid Mechanics, 2009. **640**: p. 55-77.
18. Wallau, W., et al., *Electric Field Driven Separation of Oil-water Mixtures: Model Development*, in *Computer Aided Chemical Engineering*, P.S.V. Jiří Jaromír кlemeš and L. Peng Yen, Editors. 2014, Elsevier. p. 1615-1620.